Intracardiac Mapping of SAI QRST and Other Clinical Markers

A CIS II 600.446 Capstone Project, Group 11

Members: Markus Kowalsky and Sindhoora Murthy
Mentors: Dr. Larisa Tereshenko and Dr. Fady Dawoud

JOHNS HOPKINS
MEDICINE

Technical Summary

Abstract

This is a description and overview of our course project for Computer Integrated Surgery II, 600.446, taught by Dr. Russel Taylor. Our project was titled "Intracardiac Mapping of SAI QRST and Other Clinical Markers". Below, we give a detailed overview of our methods and results.

Background

General Background

Every year, approximately 800,000 people in the United States die from cardiac disease, and roughly half of this number are a result of sudden cardiac death [1]. It is well known that ventricular arrhythmias are highly lethal and are often linked to sudden cardiac death. There are two kinds of ventricular arrhythmias: ventricular tachycardia is when there is a rapid, coordinated contraction of the ventricles, and ventricular fibrillation is when there is a rapid, uncoordinated contraction of the ventricles. Ventricular tachycardia can often degenerate into ventricular fibrillation, which can quickly lead to sudden cardiac death. Therefore, having a marker that can accurately predict a patient's risk for ventricular tachyarrhythmias is essential.

Electrocardiograms (ECGs)

ECGs are a physician's primary tool for understanding the electrical activity in the heart. While they provide certain indicators for specific heart diseases, their usefulness is weakened because they are unable to localize the arrhythmogenic substrate.

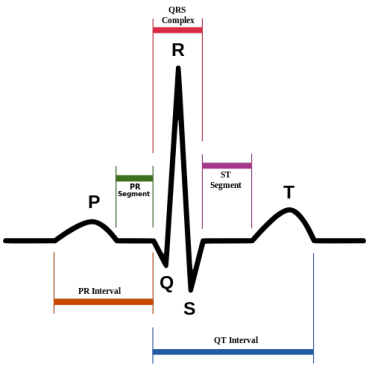

Figure 1 - shows a schematic diagram of a typical ECG wave, outlining the P, Q, R, S, and T regions of the wave, for future reference.

Various Markers of Arrhythmogenicity

SAI (Sum Absolute Integral) of the QRST interval was shown by Tereshchenko, et. al., [2] to be a good marker for a patient's ventricular arrhythmia susceptibility. The above study addressed the controversial usage of QRS width as a marker for predicting ventricular tachyarrhythmias. However, it was also shown that the predictive value of the QRS width improved if it was considered in conjunction with SAI QRST in patients implanted with primary prevention ICDs. It is believed that the QRST integral expresses the spatial heterogeneity of action potential morphology, and thus the summation of the absolute QRST integral represents the magnitude of total cardiac electrical power. In a modeling experiment by Okazaki et. al[3], the modeled myocardium was disrupted by different percentages of randomly distributed Action Potential Durations (APD). It was found through this type of modeling and simulated body surface mapping that the QRST integral was decreased with an increase in heterogeneity of APD. The researchers speculated that the reduction of QRST integral in the more heterogeneous heart models could be applied to the study of hearts in a clinical setting. A the decrease of the in QRST integral can be appropriately regarded as a consequence of increased heterogeneity of diseased hearts, as opposed to the "aligned" repolarization gradients of normal hearts[3].

Prior to this project, SAI QRST had never been studied in conjunction with body surface potential maps and inverse epicardial maps. The main goal of our project was to determine

if SAI QRST and intracardiac mapping could be combined to provide a better understanding of the electrical activity in the heart.

Body Surface Mapping and ECGi

Body surface mapping is done by placing many leads on a patient's thorax and abdomen (often done with 240 leads, but we did it with 120 leads), and recording the surface potentials from these many leads.

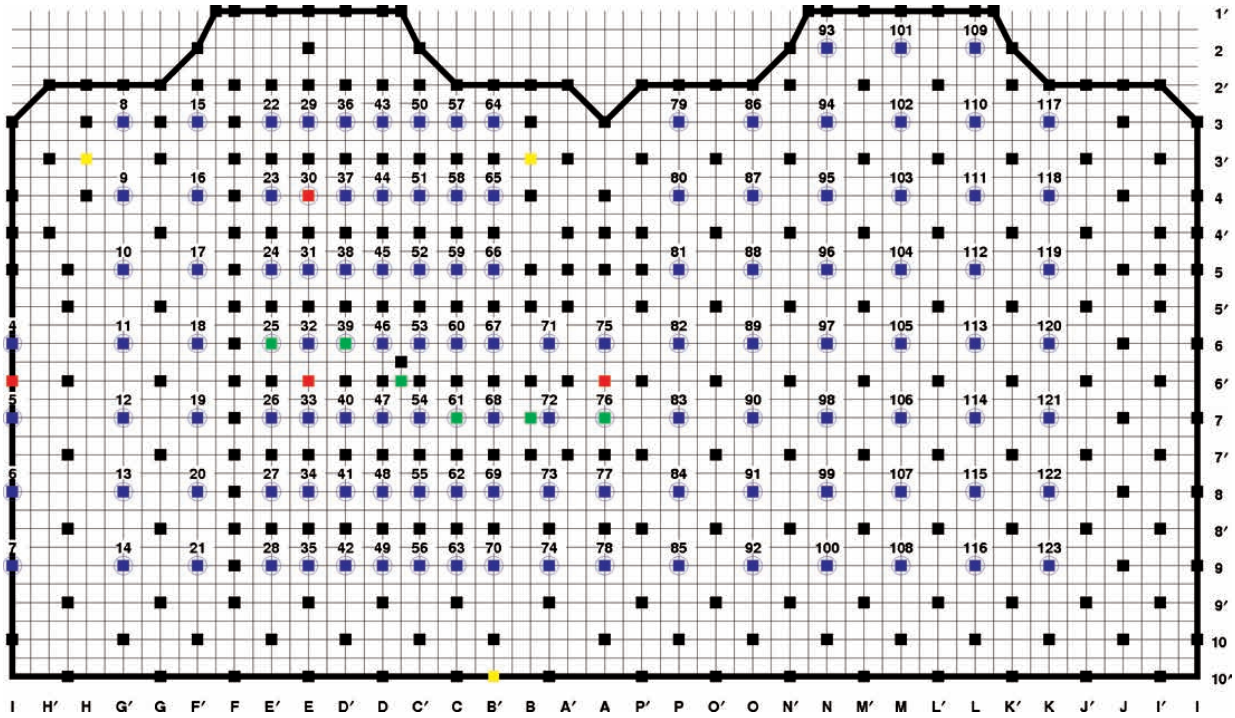

Figure 2- a standard Dalhousie array, which is similar to the electrode array that was used in our study's clinical experiments. The left side corresponds to the front of the electrode array and the right corresponds to the back of the electrode array. The green dots represent the approximate location of the standard 12-lead ECGs (only half are shown) and the red dots represent the typical placement of orthogonal leads.[8]

Additionally, ECGi consists of the additional step of taking a CT or MRI scan of the patient with the leads attached. Once completed, segmentation of the body surface, the attached

leads, and the heart can take place and a heart-torso model can be generated. The nodes of this model can then be used to plot various clinical markers.

Inverse Epicardial Heart Maps

Inverse epicardial heart maps are a way of taking the body surface information and computing an inverse solution as to what is taking place on the epicardial surface of the heart. More information on how this was accomplished is included in the Methods section of this paper.

Cardiac Resynchronization Therapy

Another use for our project was as a better marker for cardicac resynchronization therapy (CRT) device implantation. CRT device implantation is effective in approximately 60 -70% of the population but is only refunded by Medicare/Medicaid if the QRS duration (QRSd) is greater than 120 ms [4]. Recent studies, such as the study of CRT-device implantation in non-ischemic heart patients by Gosh et. al,[5] has shown that QRSd alone is not a good metric for predicting a patient success under CRT. CRT was successful in patients who were characterized by a line of conduction block between the septum and lateral left ventricular wall in inverse heart map computed using the ECGi technique.

Methods

QRS detection algorithm

This method for QRS detection was heavily adapted from Zong's Computers in Cardiology paper, published in 2003[6]. This algorithm was laid out in the paper the following way:

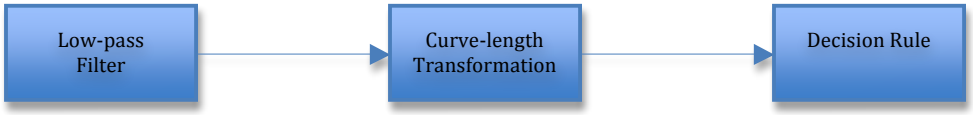

Low-pass filter

A second-order low-pass filter was used that had the following transfer function:

$$H(z) = \frac{(1 - z^{-5})^2}{(1 - z^{-1})^2}$$

And the following difference equation:

$$y[n]= 2y[n-1] –y[n-2] + x[n] -2x[n-5] +x[n-10]$$

The above filter is a low-pass filter. A high pass filter was not used in the above equation due to the fact that curve-length transformations naturally suppress high frequency components when selecting for the fiducial points.

Curve-length Transformation

The curve-length transformation consisted of taking the sum of all of the "lengths" from the current index back to a "window" w away from the current index.

$$L(w,i) = \sum_{k=i-w}^{i} \sqrt{\Delta t^2 + \Delta y_k^2}$$

Furthermore, the selection of the window width should approximately be the width of the QRS complex, so that the end of the QRS complex is detected accurately as the S point, and the point at the beginning of the length transformed signal, when the length-transformed signal is beginning to significantly rise is detected as the Q point.

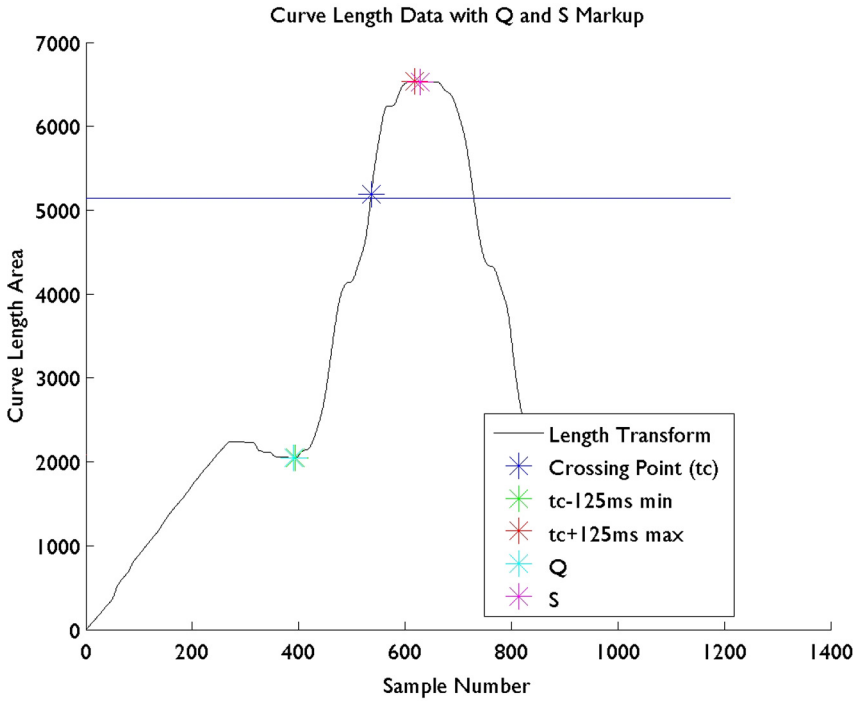

Figure 3- shows the curve length transformed graph of one of the 120 averaged beats of our data.

Decision Rule

For the single beat case, the threshold value was initially set as 120 percent of average value for the curve length transformed data within the estimated QRS complex. The estimated QRS complex was calculated visually from all leads overlaid on each other. If this threshold was never attained, then the whole method was retried for incrementally smaller thresholds until the threshold was met.

Whenever the length-transformed signal crossed the threshold value, this point was marked as a crossing point. From this point the algorithm searched back 125ms and forward 125ms to get a minimum and maximum values, which we will call Lmin and Lmax respectively. Then from the difference between Lmax and Lmin (i.e., D = Lmax – Lmin), we find where the length-transformed signal dropped from the threshold crossing point to Lmin + D/100, which we marked as the Q point, and where the length transformed signal increased from the threshold crossing point to max, which we determine as the S point. The actual Q and S points need to respectively be adjusted to -10 samples and 10 samples, respectively.

End of T-wave Detection Algorithm

This region of our methods section was heavily based on Zong's Computers in Cardiology 2006 method[7], The QRS region of the wave was originally "zeroed-out", but since our data was not necessarily at baseline before and after the QRS segment, we zeroed-out the QRS segment by simply connecting a line between the Q and the S segment and interpolating the points between them. Figure 2 shows the "zeroed-out" QRS peak from our own data:

Figure 4 – shows the "zeroed-out" QRS peak, and as you can see, the QRS peak was present from approximately the 400th index to the 600th index.

The remaining data was then fed through the length transformation. From here, a line was passed from between the peak of the length-transformed data to the end of the signal. Finally, by rotating the data between these two points, so that the secant line was horizontal, we found the minimum value. This index was then added to the index of the peak value to give the end of T fiducial point. This idea is explained in the picture below.[7]

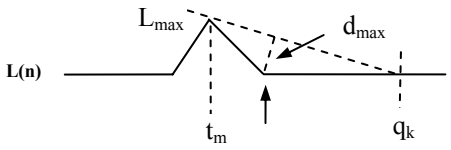

Figure 5- tilted signal minimum search[7]

Figure 5 shows how the end of the T-wave is found by tilting the signal until the diagonal line between the maximum of the length transformed signal and the baseline point is a horizontal line. Then the minimum point is found from this tilted signal. This figure does not show the tilted signal, but shows the point at which there is a minimum, or the

maximum distance between the line and the length-transformed signal. This schematic figure can be compared to that taken from real data (shown in Figure 6 below).

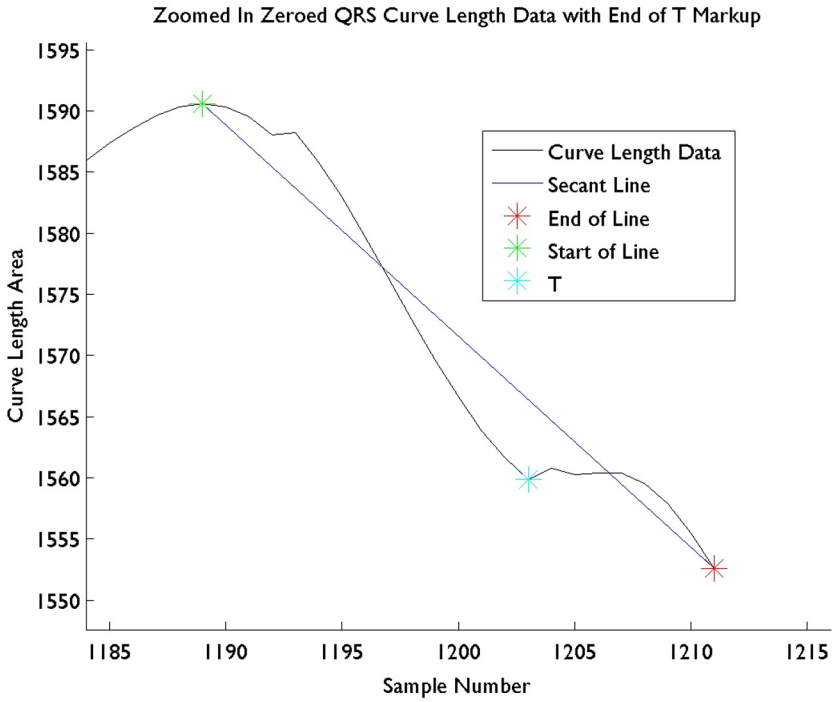

Figure 6- showing the tilted signal minimum search using our own data.

Figure 6 shows the peak of the length transformed signal, as well as the baseline, and the line connecting the two of them, shown here as the "secant line". The maximum distance in the tilted minimum search was calculated to be the blue point in the figure, and was therefore chosen to be the end of T-wave for this data set.

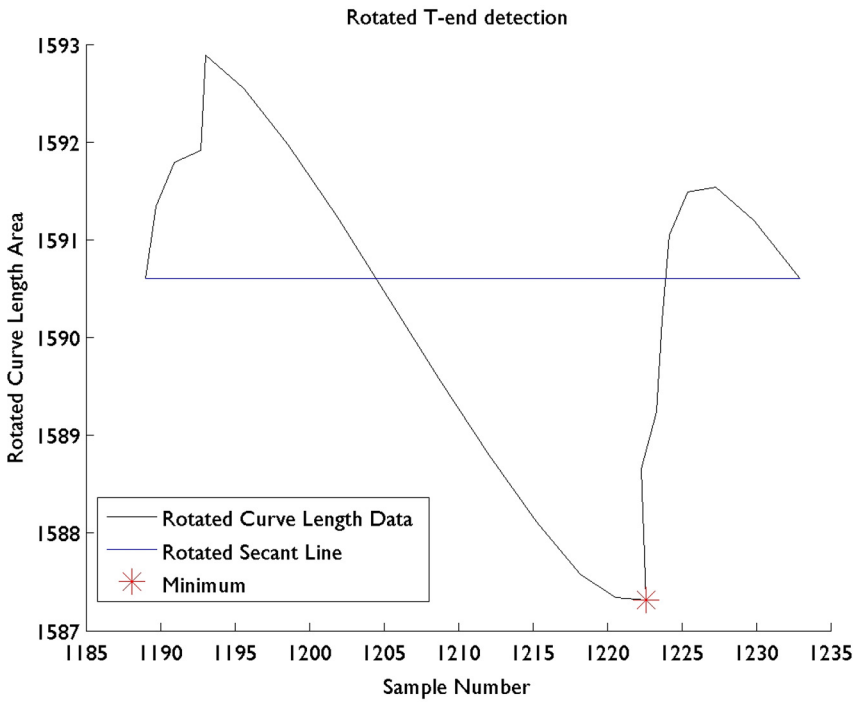

Figure 7- shows the same secant line as Figure 6 above but rotated, such that the secant line is horizontal. This figure clearly shows how the end of T is found as the tilted minimum. The red star in this figure corresponds to the T point in blue depicted in Figure 6.

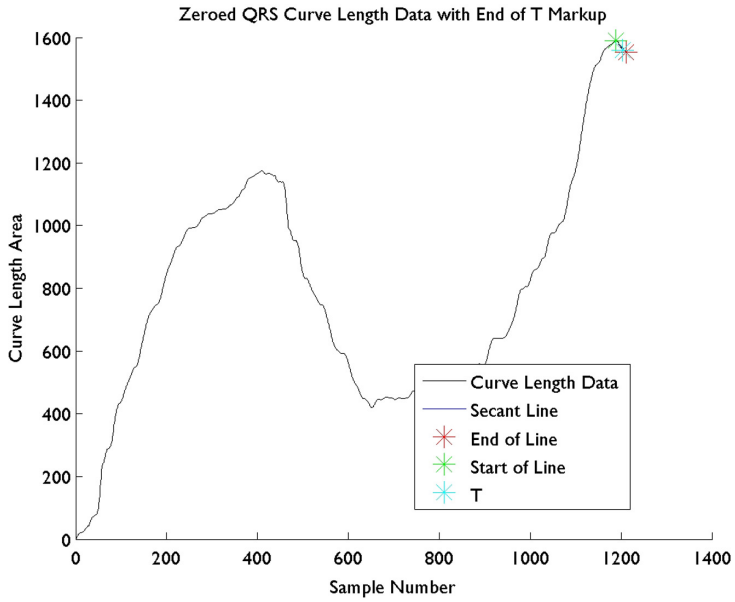

Figure 8- detection of the end of the T-wave as shown in the zeroed-out QRS curve-length transformed data.

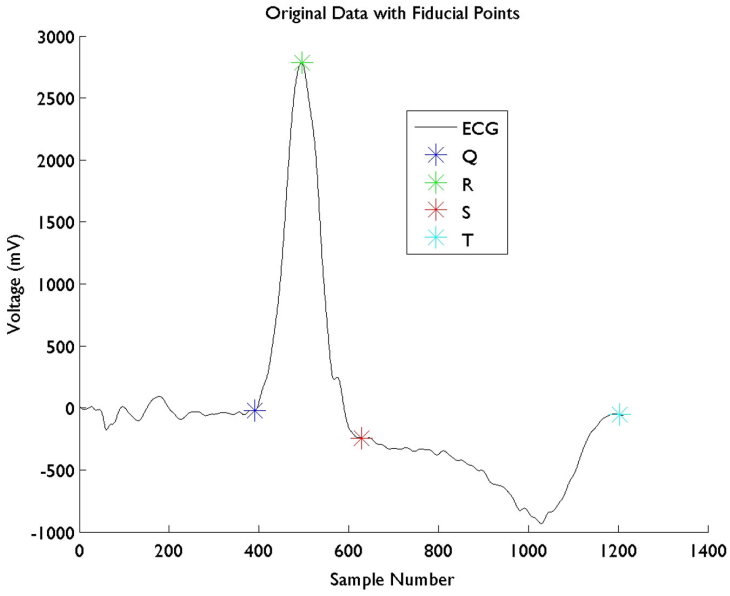

Figure 9- Showing all of the detected fiducial points as indicated by the figures and texts above.

Mapping

The body surface mapping was done the following way: ECG signals were taken from 120 leads placed on 18 strips that housed the leads as shown in Figure 10 below:

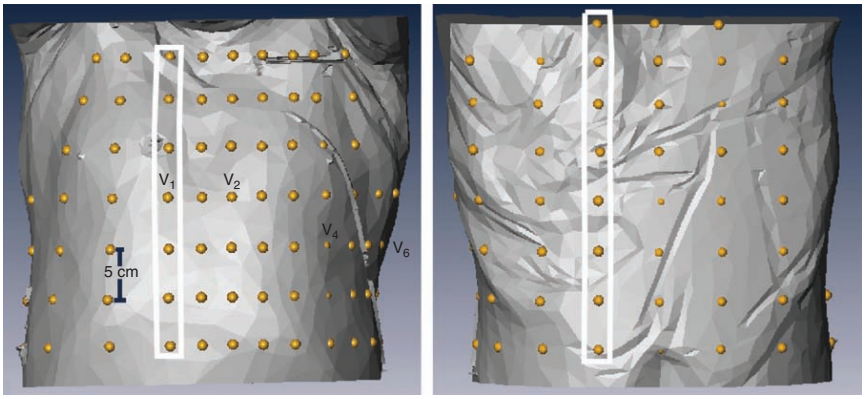

Figure 10- placement of the electrode strips as applied to patient specific model.[8]

The electrodes themselves were coated with a radiolucent Ag/AgCl and are placed in a specific arrangement on the chest. These electrodes were then connected to a 128-channel acquisition system (Active Two, BioSemi, Amsterdam, Netherlands) to record body surface potentials. The 128-channel acquisition system also filtered and digitized the channels simultaneously at a sampling rate of 2048 Hz. The data was then filtered using customized MATLAB software using a low-pass 100Hz, a high-pass 0.25 Hz and a notch 60 Hz filter. Beat averaging is done to improve the signal-to-noise ratio, as well as to obtain one averaged beat for each lead that can then be analyzed even further.

Inverse Heart Maps

The electrode labeling, and heart-torso segmentation were done by Dr. Dawoud using commercial software (AmiraTM 4.1, Mercury Computer Systems, Chelmsford, MA).

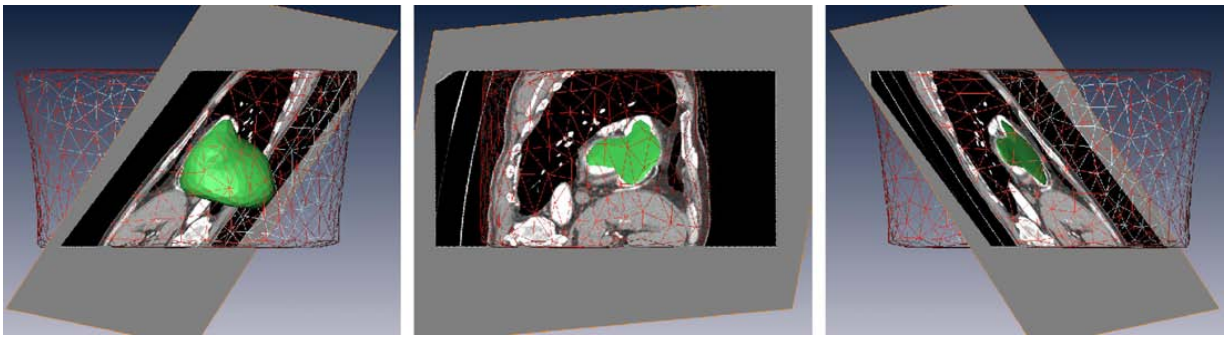

Figure 11- This figure shows the segmentation of the heart with respect to the body surface mesh. Left-most panel shows anterior view, the center panel shows the sagittal view, and the right-most panel shows the posterior view. [8]

The electric potential distribution of the heart's epicardial ventricles (V_H) are related to the body surface potential (V_B), using the following linear transformation:

$$V_B = A * V_H$$

One should be cautious about using this method, however, since small errors in the surface potentials could generate unbounded error in the solution. Inverse epicardial potentials were calculated using a method called Tikhonov regularization. The regularization parameter (t) is determined according to the following minimization problem stated below:

$$\min \{\| A\, V_H - V_B \|^2 + t \| V_H \|^2\}$$

The algorithms for calculating the inverse were developed and tested in MATLAB's computing package by our mentor Dr. Fady Dawoud.

Clinical Markers

We measured various clinical markers including absolute QRST, native QRST integral, which was simply the natural QRST integral (i.e., not the absolute value), peak-to-peak voltage of the R wave, which consisted of measuring the maximum point in the QRS wave and the minimum point in the QRS wave and finding the difference between these two voltage values.

As mentioned previously, SAI QRST is believed to represent the heterogeneity of the heart's conductive tissue, and thus, by being able to localize this metric, we can hypothesize about the functioning ability of various areas of heart tissue, and thus localize arrhythmogenic foci or areas that are scarred by myocardial infarctions.

Figures of Results:

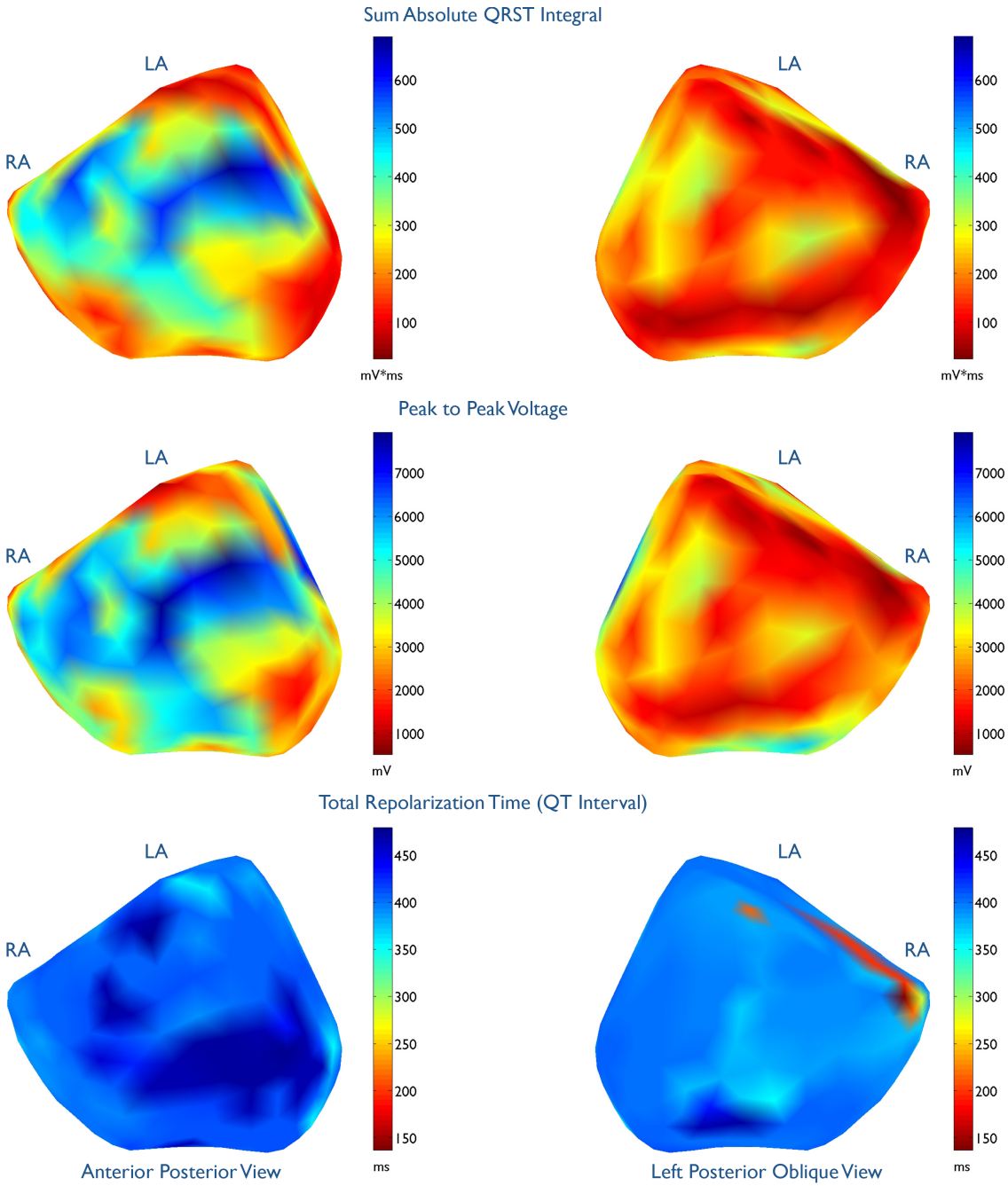

Figure 12- shows various epicardial maps of the patient whom we analyzed including SAI QRST, Peak-to-Peak Voltage, as well as the total repolarization time (QT interval).

Discussion

In relation to the scar, which was identified though an MRI scan by our mentor Dr. Tereshchenko, we found that there was a strong correlation between areas of low SAI QRST and places where a scar was present, as evidenced by that area's inability to contract, and areas of high SAI QRST and places where hypertrophied tissue was present. This gives weight to our hypothesis that low SAI QRST represents an area of slow conduction as described by Okazaki et. al.[3] However, as you can see from Figure 12- the SAI QRST maps and the peak-to-peak voltages are nearly the same, so a possible future step would be to determine the relationship between SAI QRST and other clinical markers. We believe that this method could be also used to localize scars before CRT device implantation, so that the leads can be placed optimally. Our results correlate with those of previous similar studies.[2,3,8] From Okazaki's work, which randomly modeled action potential duration heterogeneity by randomly generating different action potential duration lengths, it was found that the QRST integral (native QRST integral), curiously decreased even though action potential duration increased. This was a paradoxical finding, because traditionally a higher Q-T duration was thought to be representative of a more diseased heart. However, it has recently come to light that areas of low QRST actually represent a significant cancellation of forces due to the many misaligned electric dipoles of the heart, and that in fact, a healthy heart should normally have far more aligned electrical potentials since conduction is more heterogeneous and the voltage that is picked up on the surface of the body is a sum of the aligned electric potential and is thus larger.

Future Work

There are many avenues for future work on this project. Several of these steps will likely be implemented this summer, as Sindhoora will be working with Dr. Tereshchenko and Dr. Dawoud.

Modeling of Edema and Hypertrophy

It is well known that edema and hypertrophy affect the conduction properties of tissue, and therefore would affect the signal that is picked up on the surface of the heart. If we could somehow account for these differences while finding the inverse solution, a more accurate model may be constructed. However, there remains some contention as to whether these parameters will significantly improve the model or just increase the complexity.

Correlation with Myocardial Infarction

If we could correlate the areas that have a lower SAI QRST or peak-to-peak voltage, which shows areas of slower conduction, and we could somehow show (perhaps with overlays) how areas of the slower conduction are correlated with low SAI QRST, then that would also confirm our hypothesis that voltage or power inverse maps of the heart are a good way to non-invasively locate areas of poor conduction and therefore localize arrhythmogenic foci. This step in our future work would add evidence as to whether or not SAI QRST represents a measure of the electrical heterogeneity of the heart, and whether a three-dimensional mapping of this parameter would be useful.

Larger Sample Size

Since this an ongoing study, more data from patients is being collected, and once analyzed, should allow us to make more certain conclusions about our research.

Tool to Study Mechanism of Electrical Remodeling

Optimal lead placement must also be studied, since we will be working with data from patients before device implantation, after device implantation, and a follow-up months after implantation.

References

1. Lloyd-Jones D, Adams R, Carnethon M, et al. Heart disease and stroke statistics—2009 update: a report from the American Heart Association Statistics Committee and Stroke Statistics Subcommittee. Circulation 2009;119:480

2. Tereshchenko LG, Cheng A, Fetics BJ, et al. Ventricular arrhythmia is predicted by sum absolute QRST integral but not by QRS width. Journal of Electrocardiology 2010;43(6):548-552.

3. Okazaki O, Lux RL. Paradoxical QRST Integral Changes With V Ventricular Repolarization Dispersion. Journal of Electrocardiology 1999;32:60-69.

4. Highlights of Heart Rhythm 2004, the Annual Scientific Sessions of the Heart Rhythm Society J Am Coll Cardiol, 2004; 44: 1550-1556.

5. Ghosh S, Silva JN, Canham RM, et al. Electrophysiologic substrate and intraventricular left ventricular dyssynchrony in nonischemic heart failure patients undergoing cardiac resynchronization therapy. Heart rhythm : the official journal of the Heart Rhythm Society 2011;8(5):692-9.

6. Zong W, Moody B, Jiang D. A Robust Open-source Algorithm to Detect Onset and Duration of QRS Complexes. Computers in Cardiology 2003;30:737-740.

7. Zong W, Saeed M, Heldt T, America N, Manor B. A QT Interval Detection Algorithm Based on ECG Curve Length Transform Materials and methods. Computers in Cardiology 2006:377-380.

8. Dawoud F, Sapp JL, Clements JC, Horacek, BM. Section 1: Multimodal Imaging Evolution from Individual Imaging Modalities. In: , 2010:204-220.

Management Summary

Division of Labor

Both members worked on all aspects of the project: this included researching background information, discussion with mentors, as well as coding and testing algorithms. Markus did a lot of work with code development and validation, and Sindhoora handled the final write-up as well as researching background information and discussing with mentors.

What Was Accomplished vs. Planned

We accomplished far more than was originally planned. We essentially added two more milestones to our initial plan and deleted milestone 2 since it was no longer a relevant step in our plan. Below is a diagram of both our initial plan as well as our modified plan.

Initial Plan:

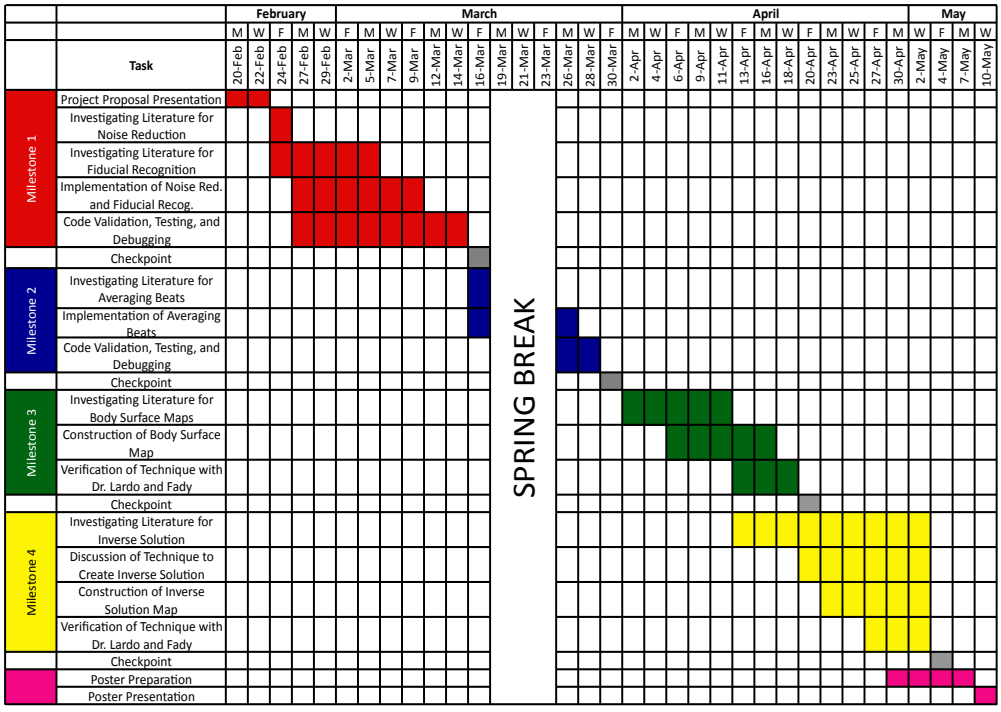

Final Plan:

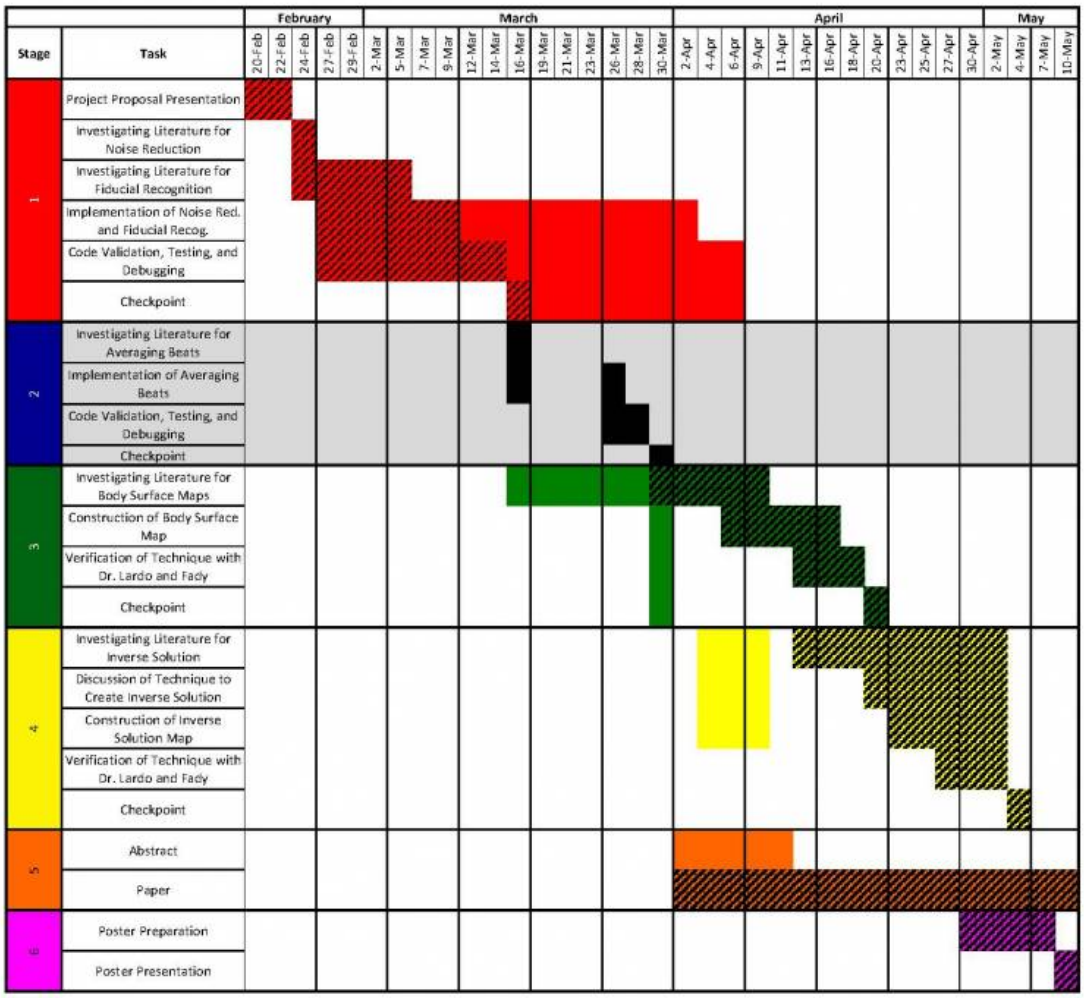

Future Work

As discussed above, this project will be continued in the summer since Sindhoora will be on campus this summer, and will be working with Dr. Tereshchenko and Dr. Dawoud. Possible areas of future work, are outlined in greater detail above, but include modeling of edema and hypertrophy, correlation of location of lower SAI QRST with myocardial infarction, as well as exploring the possibility that this technology could also be used to study the mechanism behind the phenomenon of electrical remodeling.

Lessons Learned

- Areas of low SAI QRST corresponded to areas of scar and areas of high SAI QRST correspond with hypertrophied tissue

- Finding fiducial points is difficult to completely automate with only a single beat as many existing methods are not valid for singular beats
- Small errors in recording equipment can lead to unbounded errors in the metrics measured, therefore we must do additional testing to validate whether points of singularity are artifacts of random variability in the system or if they actually represent heterogeneous conduction and dispersion.

All of the code is uploaded onto the website.